Archaean and Early Proterozoic units around northern Gulf of Bothnia: interpretation of wide-angle data from Sweden

Karsten Gohl and Laust B. Pedersen

Dept. of Geophysics, Solid Earth Physics, Uppsala University, Box 556, S-75122 Uppsala, Sweden

SUMMARY

Seismic wide-angle observations were used to derive a velocity/depth model along BABEL Profile 2. The location of well resolved wide-angle reflectors is consistent with most of the reflectivity pattern in the CDP data. We derived a velocity distribution that is consistent with the model of a Proterozoic subduction process in the northern part of the Gulf of Bothnia, its associated formation of a thick metasedimentary fore-arc basin on top of the subducted slab and the generation of intercalated mafic and metasedimentary sequences above a remnant oceanic crust.

1 INTRODUCTION

The Baltic shield of the northern Gulf of Bothnia consists of the Proterozoic Central and Northern Svecofennian Subprovinces and the Archaean Karelides (Gorbatschev & Gaal 1987). The BABEL reflection profiles 2, 3 and 4 revealed significant reflection characteristics related to the tectonic evolution of the Svecofennian subprovinces and the Karelides. The seismic data suggest a Proterozoic subduction that lead to the generation of the Central and Northern Svecofennian subprovinces (BABEL Working Group 1990, 1992). To supply important information on the seismic velocity field, we inverted wide-angle travel times from land stations that recorded the air-gun shooting of profile 2. By comparing the velocity model with the normal-incidence reflection data, we derived a possible geologic model for a Proterozoic subduction process and the accretion of an island arc complex onto the Archaean Karelides.

2 WIDE-ANGLE RECORDINGS OF BABEL PROFILE 2

The wide-angle data described here include air-gun recordings from stations F05, 201, 203 and 206 (Fig. 1). All instruments recorded vertical and both horizontal components. We trace-edited and filtered (5–25 Hz) the recordings and applied a predictive deconvolution operator with an operator length of 1000 ms, a prediction lag of 125 ms and an application gate starting at the onset of the first arrival. Most recordings show strong first arrivals (Pg and Sg), several mid-crustal phases and high-amplitude P- and S-wave reflections from the Moho (PmP and SmS). The strongest Moho reflections are observed at critical and post-critical distance (Fig. 2). There is a lack of distinct, continuous Moho arrivals at short offsets. Recordings from stations F05 and 201 (Fig. 2) contain sequences of coherent reflection phases from the middle to lower crust and the upper mantle. Two-way travel time and large move-out indicate that these reflectors coincide with series of north-dipping reflectors observed in both the normal-incidence CDP and wide-angle data recorded from a multi-channel array (station 202) close to station 201 (Lindsey & Snyder 1992).

3 TWO-DIMENSIONAL TRAVEL TIME INVERSION

We used a 2-D travel time inversion routine (Zelt & Smith 1992) to derive a velocity model based on phase picks from the recordings described above. The inversion method enabled us to calculate resolution kernels for the independent parameters named here as boundary and velocity nodes. The model was parameterized by a series of layers consisting of trapezoidal blocks with velocities linearly interpolated between nodes. The block size depended on the confidence of which phases were picked and ranged between 10 and 40 km horizontally. The calculated resolution, of course, does not take into account contingent phase mis-identification and possible 3-D effects but is valid as a relative estimation of uncertainties within the 2-D model.

The contour plot of the P-wave velocity/depth model along profile 2 (Fig. 3) shows the distribution of the velocity field with tendencies toward lower and higher velocities. Wide-angle reflectors modeled with depth uncertainties smaller than 1.5 km are indicated by white lines. The Moho depth is estimated to be 43 to 47 km in

in: Meissner, R., D. Snyder, N. Balling and E. Staroste (eds.), *The BABEL Project, First Status Report*, pp. 47-50, Commission of the European Communities, Directorate-General XII, Brussels, 1992.

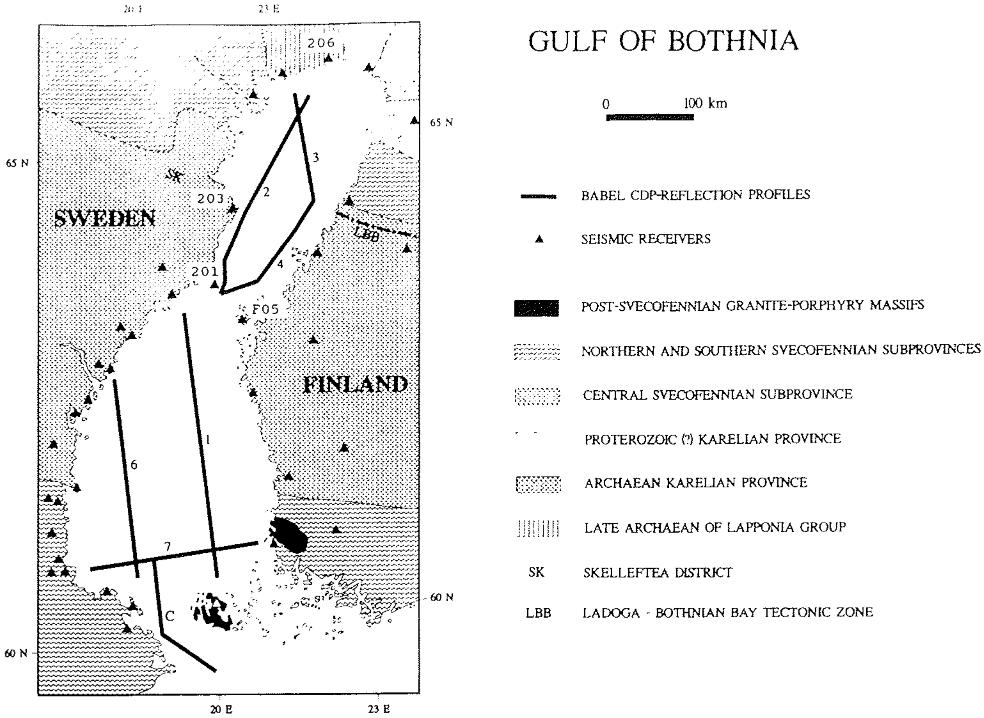

Figure 1. Geologic overview map of the Gulf of Bothnia with location of the seismic BABEL profiles and land stations (triangles). Geologic features are outlined after Gorbatschev & Gaal (1987).

the center of the profile. North-dipping interfaces dominate the southern part of the profile. They range from the upper middle crust down to the upper mantle. The P-wave velocity distribution contours follow the boundaries which, in zones of low resolution at the edges of the model, might be an effect of choosing constant initial velocities along the individual layers. There is a slight decrease in average velocity in the middle crust between 50 and 90 km horizontal distance compared to similar depths in other parts of the model. Velocities in the lowermost crust reach values of 7.0 to 7.6 km/s. The velocity resolution, however, is poor throughout the lower crust. A remarkable result is the modeling of a zone of anomalously low velocities of 7.6–7.8 km/s at about 43 to 50 km depth in the southern half of the model below a wide-angle reflector that was previously believed to be

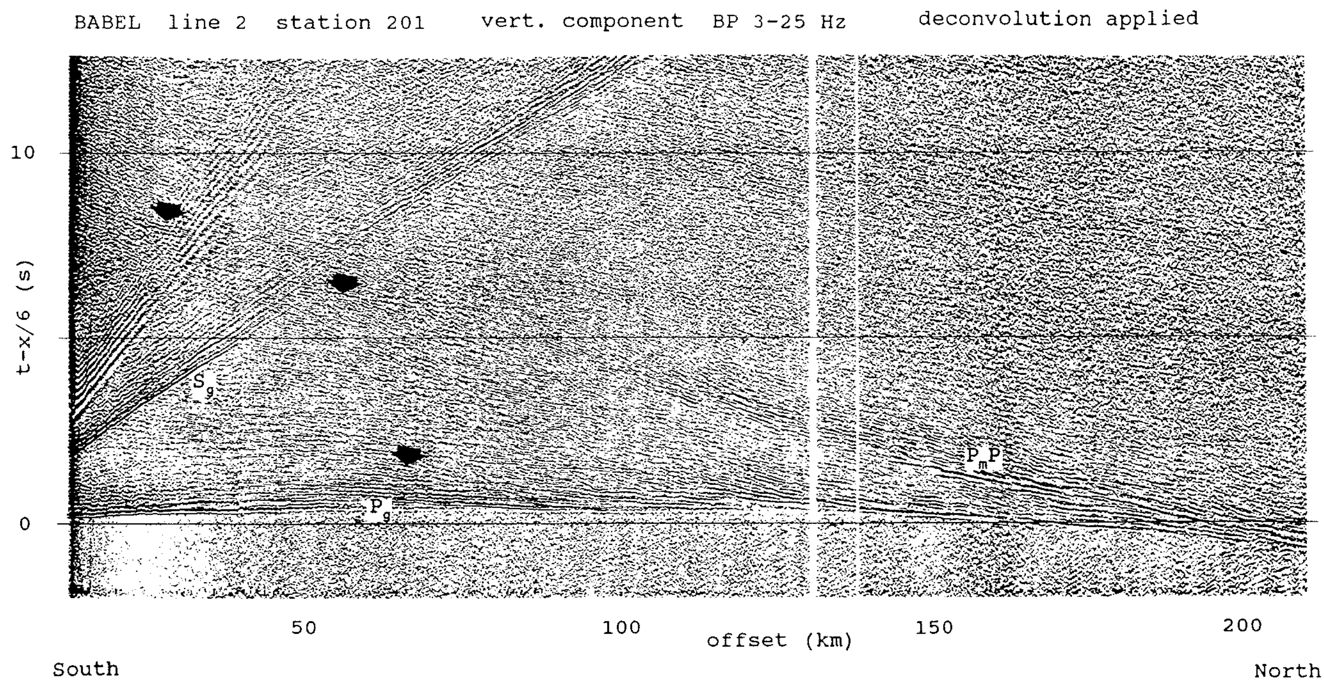

Figure 2. Receiver record of station 201 and shot profile 2. Shown are vertical component traces with major phases indicated. Note the high-amplitude Moho reflections (PmP) and mid- to lower crustal reflectors (arrows) indicating north-dipping structures in the southern part of profile 2.

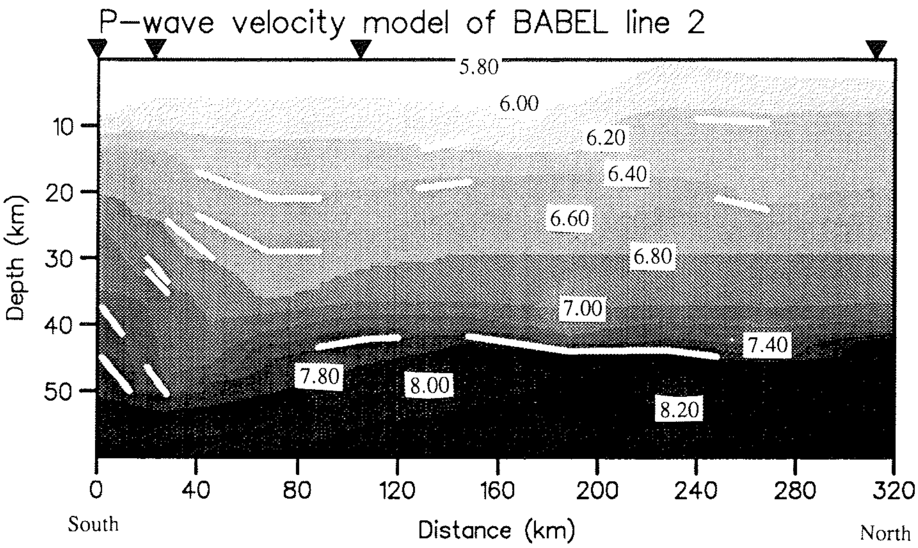

Figure 3. Contour plot of the velocity/depth distribution along profile 2 derived from 2-D travel time inversion. The location of the used stations F05, 201, 203 and 206 is indicated by triangles on top. The white lines represent wide-angle reflectors.

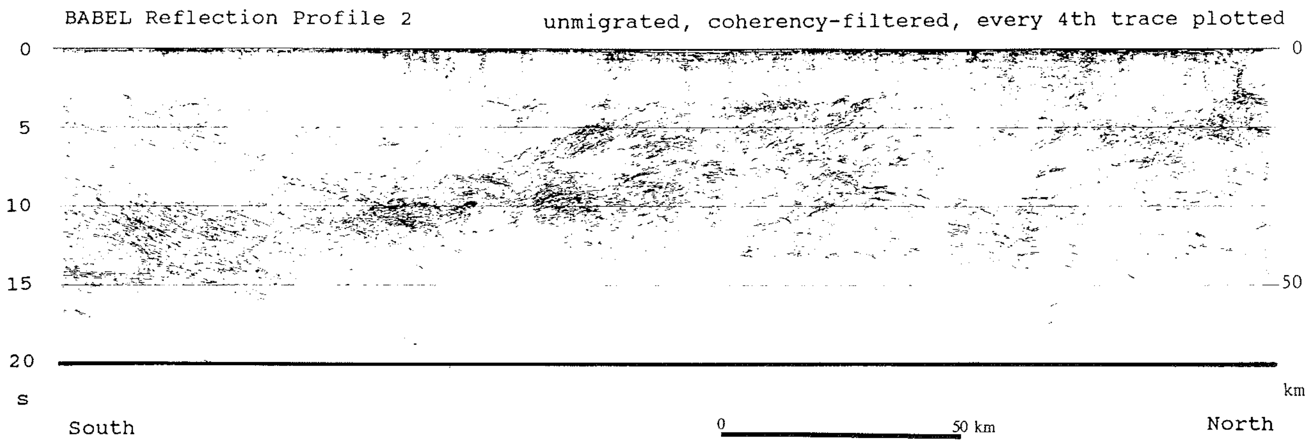

Figure 4. Coherency-filtered final stack of CDP profile 2. The filter is based on semblance calculation of nine adjacent traces (900 m) within ±30° dip. Note the coincidence in position of most wide-angle reflectors (Fig. 3) with reflection zones and/or change in reflectivity patterns of the CDP stack.

the Moho. Due to reversed observation of Pn phases from stations F05 and 206, the velocities are resolved within an uncertainty of about 0.1 km/s.

4 DISCUSSION OF VELOCITY MODEL

We compared the P-wave velocity/depth model derived from wide-angle data with the final stack of the CDP reflection profile. To enhance zones of coherent reflectors, we applied a coherency filter to the CDP data based on semblance calculation (Fig. 4). Some of the wide-angle reflectors coincide in position with reflective zones, i.e. within the bands of north-dipping reflectors in the southern part of the reflection profile. Others are located in areas where the seismic character changes from high to low reflectivity, i.e. at the base of the crust. The upper crust is seismically transparent throughout the section. This transparency and seismic velocities between 5.8 and 6.2 km/s may indicate the existence of major granitic plutons down to about 10 km depth.

Mid-crustal north-dipping reflectors to the south and south-dipping reflectors to the center of the profile enclose an area of low reflectivity coinciding with a decrease in average velocity. If the major north-dipping structures in the upper mantle are interpreted as remnants of a subducted slab (BABEL Working Group 1990, 1992), the formation of a thick metasedimentary fore-arc basin on top of that slab is likely and supported by the reflectivity pattern and velocity distribution.

Due to the low velocity resolution, an estimation of rock composition within the zone of north-dipping reflectors is not reliable. This zone has to be interpreted solely with respect to its reflectivity character. Intercalated mafic and metasediments that were scraped off during active subduction and now lie on top of the remnant oceanic crust might be responsible for large impedance contrasts and/or interference effects. Speculative, but reasonable is the implementation of a second subduction zone southwest of the previously described one. A series of upper mantle reflectors at the southernmost part of profile 2 show evidence for that.

The area above the subducted slab of oceanic crust might be filled with a mixture of mafic and ultramafic cumulates responsible for velocities of 7.6 to 7.8 km/s which are lower than normal cratonic upper mantle velocities. That implies a crust-mantle boundary that is not a sharp discontinuity but rather a thick transition zone in the southern part of profile 2.

Mid-crustal south-dipping reflection zones in the northern half of profile 2 indicate possible southward continuations of the Northern Svecofennian Subprovince and the Archaean underneath the Central Svecofennian Subprovince. The loss of reflectivity and the abundance of granitic plutons in the upper crust make a correlation with surface observations of province boundaries difficult.

REFERENCES

BABEL Working Group, 1990. Evidence for early Proterozoic plate tectonics from seismic reflection profiles in the Baltic shield, *Nature*, **348**, 34–38.

BABEL Working Group, 1992. Integrated seismic studies of the Baltic shield using data in the Gulf of Bothnia region, *Geophys. J. Int.*, in press.

Gorbatschev, R. & Gaal, G., 1987. The Precambrian history of the Baltic shield, in *Proterozoic Lithospheric Evolution*, AGU Geodynamics Series, **17**, pp.149–158, ed. Kröner, A., Washington, D.C.

Lindsey, G. & Snyder, D., 1992. Pre-critical wide-angle reflections on line 2: images of a 1.8 Ga suture zone, this volume.

Zelt, C.A. & Smith, R.B., 1992. Seismic travel time inversion for 2-D crustal velocity structure, *Geophys. J. Int.*, **108**,